J|A|C|S
ARTICLES
Published on Web 02/19/2004

# Crystal Structures and Spectroscopic Characterization of Radical Cations and Dications of Oligothiophenes Stabilized by Annelation with Bicyclo[2.2.2]octene Units: Sterically Segregated Cationic Oligothiophenes

Tohru Nishinaga, Atsushi Wakamiya, Daisuke Yamazaki, and Koichi Komatsu*

*Contribution from the Institute for Chemical Research, Kyoto University, Uji, Kyoto 611-0011, Japan*

Received November 5, 2003; E-mail: komatsu@scl.kyoto-u.ac.jp

***Abstract:*** The remarkably stable $SbF_6^-$ salts of the radical cations of bithiophene **1**(2T) and terthiophene **1**(3T), completely surrounded by bicyclo[2.2.2]octene (BCO) units, were obtained by one-electron oxidation of the neutral precursors with $NO^+SbF_6^-$, and their solid-state structures were determined by X-ray crystallography. In these radical cations, the presence of quinoidal character was apparent, as shown by the increased planarity and by comparison of the bond lengths with those of the neutral precursors. The shortest intermolecular $\pi-\pi$ distances in the crystal structure of **1**(2T)$^{\bullet+}SbF_6^-$ (distance between two $sp^2$ carbon atoms, 4.89 Å) and **1**(3T)$^{\bullet+}SbF_6^-$ (distance between an $sp^2$ carbon and a sulfur atom, 3.58 Å) were found to be longer than the sums of the van der Waals radii of the corresponding atoms. In accord with this, no apparent change was observed in ESR and UV−vis−NIR spectra of solutions of **1**(2T)$^{\bullet+}$ and **1**(3T)$^{\bullet+}$ upon lowering the temperature, indicating that the $\pi$- (or $\sigma$-) dimer formation is inhibited in solution as well as in the solid state. The dications **1**$(2T)^{2+}$ and **1**$(3T)^{2+}$ were generated with the stronger oxidant $SbF_5$ in $CH_2Cl_2$ at −40 °C and characterized by NMR spectroscopy. In the $^1H$ NMR spectra, two conformers were observed for each dication of both **1**$(2T)^{2+}$ (transoid (*t*) and cisoid (*c*)) and **1**$(3T)^{2+}$ (*t*,*t* and *c*,*t*) at room temperature due to the high rotational barrier around the inter-ring bond(s) between thiophene rings, which was caused by the enhanced double bond character of these bonds following two-electron oxidation. This is supported by DFT calculations (B3LYP/6-31G(d)), which predicted the rotational barriers in the dications of unsubstituted bithiophene and terthiophene to be 27.6 and 22.9 kcal $mol^{-1}$, respectively. In the case of quaterthiophene and sexithiophene surrounded by BCO frameworks **1**(4T) and **1**(6T), oxidation with even one molar equivalent of $NO^+SbF_6^-$ afforded the dication salts **1**$(4T)^{2+}2SbF_6^-$ and **1**$(6T)^{2+}2SbF_6^-$, which were isolated as stable single crystals and allowed the X-ray crystallography. In their crystal structures, the cationic $\pi$-systems became planar again due to the great contribution of quinoidal resonance structures, and the $\pi$-systems, which were arrayed in a parallel geometry, were also segregated by the steric effect of BCO units. The degree and tendency of changes in the bond lengths of thiophene rings of **1**$(4T)^{2+}$ and **1**$(6T)^{2+}$ as compared with neutral precursors were similar to those of **1**(2T)$^{\bullet+}SbF_6^-$ and **1**(3T)$^{\bullet+}SbF_6^-$, respectively, implying that the contribution of quinoidal character is modulated by the amount of positive charge per thiophene unit.

## Introduction

In the pursuit of the conduction mechanism of p-doped polythiophenes and related conductive polymers, radical cations and dications of oligothiophenes[1] have been intensively investigated as models for polarons and bipolarons[2] of polythiophenes. Although such oligomer approaches have contributed to refining the understanding of the electronic properties of the corresponding polymers, the interpretation of the fundamental nature of the charge carrier is still controversial. Because of the ESR-inactive nature of the doped polythiophenes, not polarons (radical cations) but bipolarons (dications) were considered to serve as the charge carriers for the doped polythiophenes in early works.[3] However, in 1992, Miller and co-workers reported the reversible dimerization of a terthiophene radical cation derivative and proposed that the diamagnetic dimer dications formed from the interchain $\pi$-stacks of radical cation (i.e., "$\pi$-dimers") can be alternatives to bipolarons.[4] Following this influential pro-

(1) For recent reviews, see: (a) Hotta, S. In *Handbook of Organic Conductive Molecules and Polymers*; Nalwa, H. S., Ed.; Wiley: Chichester, 1997; Vol. 2, Chapter 8. (b) Baüerle, P. In *Electronic Materials: The Oligomer Approach*; Müllen, K., Wegner, G., Eds.; Wiley-VCH: Weinheim, 1998; Chapter 2. (c) *Handbook of Oligo- and Polythiophenes*; Fichou, D., Ed.; Wiley-VCH: Weinheim, 1999. (d) Otsubo, T.; Aso, Y.; Takimiya, K. *Bull. Chem. Soc. Jpn.* **2001**, *74*, 1789.

(2) (a) Brédas, J. L.; Street, G. B. *Acc. Chem. Res.* **1985**, *18*, 309. (b) Heeger, A. J.; Kivelson, S.; Schrieffer, J. R.; Su, W.-P. *Rev. Mod. Phys.* **1988**, *781*, 60.

(3) For example, see: (a) Kaneto, K.; Hayashi, S.; Ura, S.; Yoshino, K. *J. Phys. Soc. Jpn.* **1985**, *54*, 1146. (b) Chen, J.; Heeger, A. J.; Wudl, F. *Solid State Commun.* **1986**, *58*, 251.

(4) (a) Hill, M. G.; Mann, K. R.; Miller, L. L.; Penneau, J.-F. *J. Am. Chem. Soc.* **1992**, *114*, 2728. (b) Hill, M. G.; Penneau, J.-F.; Zinger, B.; Mann, K. R.; Miller, L. L. *Chem. Mater.* **1992**, *4*, 1106.

10.1021/ja039434v CCC: $27.50 

posal[4] challenging the general perception of polaron/biporalon theory, reversible dimerizations of radical cations have been reported on a wide variety of $\pi$-conjugated oligomers, including not only substituted oligothiophenes[5−9] but also other systems such as oligopyrroles,[10] oligo(phenylenevinylene)s,[11] and mixed oligomers composed of benzene, thiophene, or pyrrole units.[12]

Whereas these reports assumed $\pi$-dimer formation for the interchain interaction of radical cations, Heinze proposed $\sigma$-bond formation between two radical cation chains (i.e., $\sigma$-dimer formation) on the basis of the results of an electrochemical study on radical cations of diphenylpolyenes, 3,3′,5,5′-tetramethylbithiophene, and oligo(phenylenevinylene)s.[13] This $\sigma$-dimer formation was also observed by low-temperature NMR measurement of the radical cation of 5,5′-diphenyl-3,3′,4,4′-tetramethoxybipyrrole in solution, although in the solid state the radical cation salts showed the $\pi$-stacked structure without any $\sigma$-bond formation.[14]

On the other hand, Janssen and co-workers reported that a bipolaron (i.e., dication) tends to be separated into two independent polarons (i.e., radical cations) as the chain length increases.[8a] On the basis of the results of UV−vis−NIR spectroscopy, the ESR-inactive character, and theoretical considerations, they claimed that the "two-polaron state" in a single chain can be a singlet ground state and that the assumption of intermolecular $\pi$- (or $\sigma$-) dimer formation would not be necessary to interpret the diamagnetic properties for longer oligothiophene dications.[15]

Aside from the Janssen's claim, dimerization is considered to be a general property for cationic $\pi$-conjugated oligomers in solution. However, in most of the studies supporting such a property, the intermolecular interaction has been discussed only on the basis of spectral means, i.e., mostly UV−vis−NIR spectroscopy, using mixtures of neutral and cationic species without isolation of the cationic species in pure form. In addition, although the $\pi$-stacked structures of radical cations of rather shorter-chain oligomers such as 3′,4′-dibutyl-5,5″-diphenylterthiophene[16] and 5,5′-diphenyl-3,3′,4,4′-tetramethoxybipyrrole[14] have been determined by X-ray crystallography, the possibility of dimerization in the solid state still remains unclear for the longer-chain oligomers.

This ambiguity can be ascribed to the lack of information about the unimolecular electronic structure of longer oligothiophenes dications. An important step toward elucidating such a unimolecular property would be the establishment of a model structure that can make the $\pi$-system sterically hindered so that the dimerization of cationic oligothiophenes can be avoided. In addition, the presence of sterically demanding substituents,[17] which causes segregation of each cationic $\pi$-conjugated system, can be expected to work as an intermolecular insulator when the system is used as a part of molecular-scale devices,[18] which are currently attracting considerable attention from the viewpoint of nanotechnology. Dendrimer units seem to be one of the promising candidates for such substituents, but no apparent evidence for steric inhibition of the dimerization could be obtained for oligothiophenes functionalized with poly(benzyl ether)-type dendrons attached at the α-positions of both ends, when it was positively doped.[8b] As another example of the structural control of dimerization in cationic $\pi$-conjugated oligomers, substitution at all the $\beta$-positions of thiophene rings with octyl groups has been reported to inhibit the dimerization of the radical cation of a thienylenevinylene tetramer.[19] However, this kind of alkyl-group substitution at all $\beta$-positions may not be suitable for planarization of oligothiophenes because the steric hindrance between the alkyl chain and the atoms in an adjacent thiophene unit can cause significant distortion of the cationic oligothiophene $\pi$-system.

In comparison to those structural modifications described above, annelation of all the thiophene rings with bicyclo[2.2.2]-octene (abbreviated as BCO) is expected to satisfy the requirement of steric protection without severe distortion of the cationic oligothiophene $\pi$-system, since the angle of C($\beta$)−C($\beta'$)−C(BCO-bridgehead) in the $\beta,\beta'$-BCO-annelated thiophene ring should be smaller than the corresponding angle in the one having an alkyl side chain.[20] Thus, we designed and synthesized a series of oligothiophene annelated with BCO units, **1**(*n*T), ($n$ = 2, 3, 4, 6).[21]

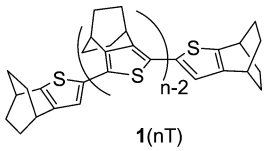


**1**(nT)

In addition to the steric protection of the $\pi$-systems, the structural modification with BCO units has been shown to be quite effective for the stabilization of cationic $\pi$-systems owing to electronic effects such as inductive and $\sigma-\pi$ conjugative effects as well as the so-called "Bredt's rule protection".[22] Actually, we have succeeded in isolation and X-ray structural

(5) Yu, Y.; Gunic, E.; Zinger, B.; Miller, L. L. *J. Am. Chem. Soc.* **1996**, *118*, 1013.
(6) (a) Bäuerle, P.; Segelbacher, U.; Gaudl, K.-U.; Huttenlocher, D.; Mehring, M. *Angew. Chem., Int. Ed. Engl.* **1993**, *32*, 76. (b) Bäuerle, P.; Segelbacher, U.; Maier, A.; Mehring, M. *J. Am. Chem. Soc.* **1993**, *115*, 5, 10217. (c) Bäuerle, P.; Fisher, T.; Bidlingmeier, B.; Stabel, A.; Rabe, J. *Angew. Chem., Int. Ed. Engl.* **1995**, *34*, 303.
(7) Nessakh, B.; Horowitz, G.; Garnier, F.; Deloffre, F.; Strivastava, P.; Yassar, A. *J. Electroanal. Chem.* **1995**, *399*, 97.
(8) (a) van Haare, J. A. E. H.; Havinga, E. E.; van Dongen, J. L. J.; Janssen, R. A. J.; Cornil, J.; Brédas, J.-L. *Chem. Eur. J.* **1998**, *4*, 1509. (b) Apperloo, J. J.; Janssen, R. A. J.; Malenfant, P. R. L.; Groenendaal, L.; Fréchet, J. M. J. *J. Am. Chem. Soc.* **2000**, *122*, 7042. (c) Apperloo, J. J.; Groenendaal, L.; Verheyen, H.; Jayakannan, M.; Janssen, R. A. J.; Dkhissi, A.; Beljonne, D.; Lazzaroni, R.; Brédas, J.-L. *Chem. Eur. J.* **2002**, *8*, 2384.
(9) Nakanishi, H.; Sumi, N.; Ueno, S.; Takimiya, K.; Aso, Y.; Otsubo, T.; Komaguchi, K.; Shiotani, M.; Ohta, N. *Synth. Met.* **2001**, *119*, 413.
(10) van Haare, J. A. E. H.; Groenendaal, L.; Havinga, E. E.; Janssen, R. A. J.; Meijer, E. W. *Angew. Chem., Int. Ed. Engl.* **1996**, *35*, 638.
(11) Sakamoto A.; Furukawa, Y.; Tasumi, M. *J. Phys. Chem. B* **1997**, *101*, 1726.
(12) (a) van Haare, J. A. E. H.; Groenendaal, L.; Havinga, E. E.; Meijer, E. W.; Janssen, R. A. J. *Synth. Met.* **1997**, *85*, 1091. (b) van Haare, J. A. E. H.; van Boxtel, M.; Janssen, R. A. J. *Chem. Mater.* **1998**, *10*, 1166.
(13) (a) Smie, A.; Heinze, J. *Angew. Chem., Int. Ed. Engl.* **1997**, *36*, 363. (b) Tschuncky, P.; Heinze, J.; Smie, A.; Engelmann, G.; Kossmehl, G. *J. Electroanal. Chem.* **1997**, *433*, 223. (c) Heinze, J.; Tschuncky, P.; Smie, A. *J. Solid State Electrochem.* **1998**, *2*, 102.
(14) Merz, A.; Kronberger, J.; Dunsch, L.; Neudeck, A.; Petr, A.; Parkanyi, L. *Angew. Chem., Int. Ed.* **1999**, *38*, 1442.
(15) However, there was also a claim that the separated polarons from different two chains could form $\pi$-dimers: see ref 7.
(16) (a) Graf, D. D.; Campbell, J. P.; Miller, L. L.; Mann, K. R. *J. Am. Chem. Soc.* **1996**, *118*, 5480. (b) Graf, D. D.; Duan, R. G.; Campbell, J. P.; Miller, L. L.; Mann, K. R. *J. Am. Chem. Soc.* **1997**, *119*, 5888.
(17) See also: Tanaka, S.; Yamashita, Y. *Synth. Met.* **2001**, *119*, 67.
(18) For reviews, see for example: (a) Tour, J. M. *Acc. Chem. Res.* **2000**, *33*, 791. (b) Joachim, C.; Gimzewski, J. K.; Aviram, A. *Nature* **2000**, *408*, 541. (c) Nitzan, A.; Ratner, M. A. *Science* **2003**, *300*, 1384.
(19) Levillain, E.; Roncali, J. *J. Am. Chem. Soc.* **1999**, *121*, 8760.
(20) Similarly, in oligothiophenes annelated with substituted cyclopentene units at the $\beta,\beta'$-position, no severe distortion was observed. See: Izumi, T.; Kobashi, S.; Takimiya, K.; Aso, Y.; Otsubo, T. *J. Am. Chem. Soc.* **2003**, *125*, 5286.
(21) Wakamiya, A.; Yamazaki, D.; Nishinaga, T.; Kitagawa, T.; Komatsu, K. *J. Org. Chem.* **2003**, *68*, 8305.
(22) Komatsu, K. *Bull. Chem. Soc. Jpn.* **2001**, *74*, 407.

determination of radical cation salts and NMR observation of dications of various cyclic $\pi$-conjugated systems annelated with BCO units.[23]

As for the study of the X-ray crystal structure of cationic oligothiophene salts, only the radical cation of 3′,4′-dibutyl-5,5″-diphenylterthiophene (**2**)[16] and the dication of the $\pi$-expanded quaterthiophene **3**[24] were reported. However, no systematic study on the X-ray structure of cationic oligothiophenes has so far been made, despite its significance for the elucidation of precise structural changes in oligo- or polythiophenes upon doping. The NMR spectral study on oligothiophene dications should also be quite informative concerning their electronic properties. However, to the best of our knowledge, there has been no report on such a study, possibly due to the intrinsic instability of the dication (particularly for shorter-chain oligomers) and the difficulty in obtaining the pure sample (particularly for longer-chain oligomers).

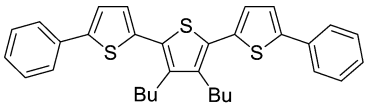


**2**

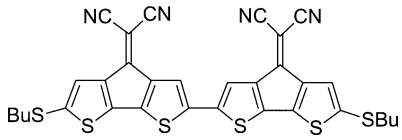


**3**

In the present paper, we describe the first well-defined and sterically segregated cationic oligothiophenes, that is, the radical cations and dications of **1**(*n*T) ($n$ = 2, 3, 4, 6), for which the $\pi$- or $\sigma$-dimerization of cationic $\pi$-systems is kinetically inhibited by steric effects of the bicyclic units and the cationic species themselves are thermodynamically stabilized by the electronic effects of the BCO units. The cationic species generated from **1**(*n*T) are expected to be good models of the unimolecular state of the partial structure of p-doped polythiophenes. Using these model systems, it has become possible to elucidate the precise electronic structures of the cationic oligothiophenes, which involve some quinoidal character, on the basis of the experimental results of X-ray crystallography and UV−vis−NIR, ESR, and NMR spectroscopy as well as the results of DFT calculations.

## Results and Discussion

**Preparation and Structural Properties of Radical Cation Salts of Bithiophene 1(2T) and Terthiophene 1(3T). (a) Bithiophene 1(2T).** The previous electrochemical study on bithiophene **1**(2T) and terthiophene **1**(3T) indicated that they can undergo reversible one-electron oxidations at considerably low potentials ($E_{1/2}$ = +0.47V vs $Fc/Fc^+$ for **1**(2T) and +0.27 V for **1**(3T)).[21] In accord with this, the chemical one-electron oxidation of **1**(2T) and **1**(3T) with 1.0 equiv of $NO^+SbF_6^-$ in $CH_2Cl_2$ under vacuum at room temperature took place smoothly. Slow diffusion of hexane into the solutions gave single crystals of **1**(2T)$^{\bullet+}SbF_6^-$ (deep green) and **1**(3T)$^{\bullet+}SbF_6^-$ (dark purple) in 61% and 73% yield, respectively (Scheme 1). These crystals were so stable that no decomposition was observed, even after the crystals were left to stand at room temperature under air for 1 month. The remarkable stability of **1**(2T)$^{\bullet+}$, owing to the end-capping with BCO units, is to be compared with the relative instability of a similar bithiophene radical cation end-capped by cyclohexene; the latter is indicated by an irreversible oxidation peak upon cyclic voltammetry of the neutral bithiophene.[6b]

***Scheme 1***

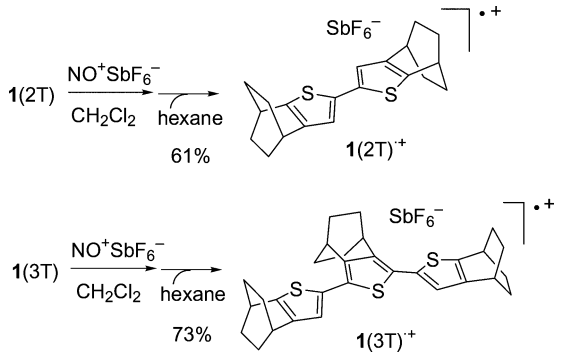


The molecular structure of **1**(2T)$^{\bullet+}SbF_6^-$ was determined by X-ray crystallography for the first time as a radical cation of bithiophenes. As shown in Figure 1, the structure of the $\pi$-system in **1**(2T)$^{\bullet+}$ is completely planarized (dihedral angle C3−C4−C5−C6, 180.0°), while that of the $\pi$-system in neutral **1**(2T)[21] is slightly twisted (174.3°). This planarization is accompanied by considerable shortening of the inter-ring bond (C4−C5, 1.398(8) Å) as compared with the same bond in **1**(2T) (1.455(3) Å). According to Pauling's bond order ($n$)−bond length ($r$) relationship,[25] using recently reported parameters,[26] the bond orders ($n_{C-C}$) of these inter-ring bonds are calculated as 1.25 for **1**(2T) and 1.52 for **1**(2T)$^{\bullet+}$. Hence, the planarization upon one-electron oxidation reflects the enhanced double bond character of the inter-ring bond. On the other hand, bonds S1−C1 (1.696(5) Å, $n_{C-S}$ = 1.60) and C2−C3 (1.371(6) Å, $n_{C-C}$ = 1.67) are shortened in **1**(2T)$^{\bullet+}$ as compared with those of **1**(2T) (1.727(3) Å ($n_{C-S}$ = 1.46) and 1.409(7) Å ($n_{C-C}$ = 1.47)), respectively), while bonds C1−C2 (1.408(6) Å, $n_{C-C}$ = 1.47), C3−C4 (1.403(6) Å, $n_{C-C}$ = 1.50), and C4−S1 (1.752(4) Å, $n_{C-S}$ = 1.37) are elongated compared with those in **1**(2T) (1.351(3) Å ($n_{C-C}$ = 1.79), 1.363(7) Å ($n_{C-C}$ = 1.71), and 1.745(2) Å ($n_{C-S}$ = 1.39), respectively). Thus, the bond order becomes higher on bonds C4−C5, C2−C3, and C1−S1 upon the one-electron oxidation of **1**(2T).

Concerning the crystal packing, the $\pi$-systems of **1**(2T)$^{\bullet+}$ are arrayed in a parallel but considerably slipped fashion, with the intermolecular distance between the $\pi$-systems being 4.89 Å (Figure 1b). Apparently, the formation of a $\pi$-dimer is inhibited by the end-capping with BCO units, even though stacking of

(23) (a) Nishinaga, T.; Komatsu, K.; Sugita, N.; Lindner, H. J.; Richter, J. *J. Am. Chem. Soc.* **1993**, *115*, 11642. (b) Nishinaga, T.; Komatsu, K.; Sugita, N. *J. Chem. Soc., Chem. Commun.* **1994**, 2319. (c) Nishinaga, T.; Wakamiya, A.; Komatsu, K. *Tetrahedron Lett.* **1999**, *40*, 4375. (d) Nishinaga, T.; Wakamiya, A.; Komatsu, K. *Chem. Commun.* **1999**, 777. (e) Matsuura, A.; Nishinaga, T.; Komatsu, K. *J. Am. Chem. Soc.* **2000**, *122*, 10007. (f) Nishinaga, T.; Inoue, R.; Matsuura, A.; Komatsu, K. *Org. Lett.* **2002**, *4*, 4117. (g) Wakamiya, A.; Nishinaga, T.; Komatsu, K. *Chem. Commun.* **2002**, 1192. (h) Wakamiya, A.; Nishinaga, T.; Komatsu, K. *J. Am. Chem. Soc.* **2002**, *124*, 15038.

(24) Kozaki, M.; Yonezawa, Y.; Okada, K. *Org. Lett.* **2002**, *4*, 4535.

(25) $n_{A-B} = \exp[(r_0 - r)/a]$, where $r_0$ and $a$ are empirical parameters: see *The Nature of the Chemical Bond and the Structure of Molecules and Crystals*; Pauling, L., Ed.; Cornell University Press: Ithaca, NY, 1960.

(26) The parameters $r_0$ = 1.521 and $a$ = 0.293 for the C−C bond and $r_0$ = 1.865 and $a$ = 0.363 for the C−S bond were used. Howard, S. T.; Lamarche, O. *J. Phys. Org. Chem.* **2003**, *16*, 133.

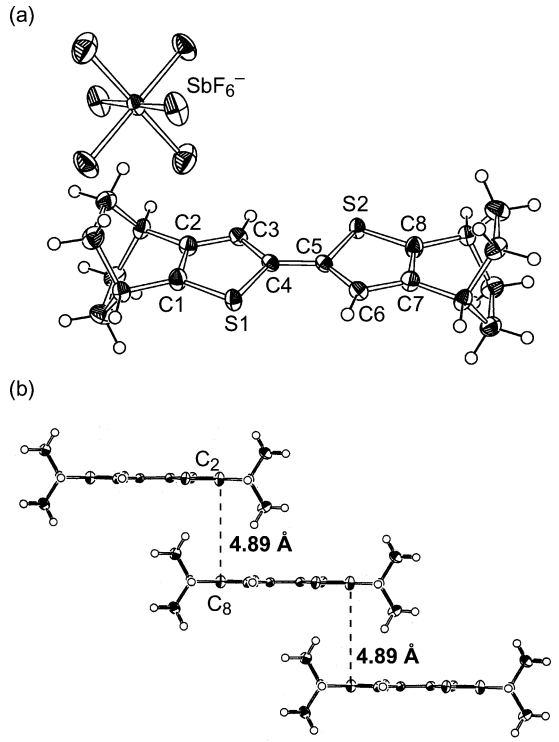


***Figure 1.*** (a) ORTEP drawing of **1**(2T)$^{\bullet+}SbF_6^-$. Thermal ellipsoids are drawn at the 50% probability level. Selected bond lengths (Å) and angles (deg): S1−C1, 1.696(5); C1−C2, 1.408(6); C2−C3, 1.371(6); C3−C4, 1.403(6); C4−S1, 1.752(4); C4−C5, 1.398(8); C1−S1−C4, 90.5(2); S1−C1−C2, 113.1(3); C1−C2−C3, 112.4(4); C2−C3−C4, 112.7(3); C3−C4−S1, 111.3(3); C3−C4−C4−C6, 180.0. (b) Crystal packing drawing; the $SbF_6^-$ ions are omitted for clarity.

the $\pi$-systems positioned at right angles to each other is reported to be possible in the case of the $\pi$-dimer of the terthiophene radical cation having such bulky substituents as phenyldimethylsilyl groups at the α-positions of both ends.[5]

Next, to clarify the electronic structure of radical cation **1**(2T)$^{\bullet+}$, a solution of **1**(2T)$^{\bullet+}SbF_6^-$ in $CH_2Cl_2$ ($1.0 \times 10^{-5}$ M) was subjected to ESR measurement at room temperature. As shown in Figure 2a, a signal with hyperfine couplings was observed. According to the calculated results on the optimized structure of **1**(2T)$^{\bullet+}$ at the UB3LYP/6-31G(d) level (Figure 2c), the spin is mainly distributed on C1 and C8 (0.2923 each), and this induces coupling with the four equivalent *anti* protons of the corresponding methylene carbons in the BCO units (H1,8$^{anti}$, $a_H = 0.19$ mT). The couplings with other protons in the BCO units were found to be negligibly small (<0.05 mT). On the other hand, the coupling with two equivalent protons directly attached to the thiophene rings (H3,6) is calculated as −0.29 mT. The simulated ESR spectrum using these calculated coupling constants was in excellent agreement with the experimental spectrum, as shown in Figure 2b, indicating the validity of the calculated spin distribution of **1**$^{\bullet+}$ by the DFT method. As also shown in Figure 2c, the positive charge is calculated to reside mostly on sulfur atoms.

Thus, the results of X-ray crystallography and ESR measurement as well as theoretical calculations are all in agreement with a significant contribution of the quinoidal resonance structures (Chart 1) to the electronic state of the bithiophene radical cation. Although similar quinoidal character in bithiophene radical cations has been described repeatedly,[27] the present work

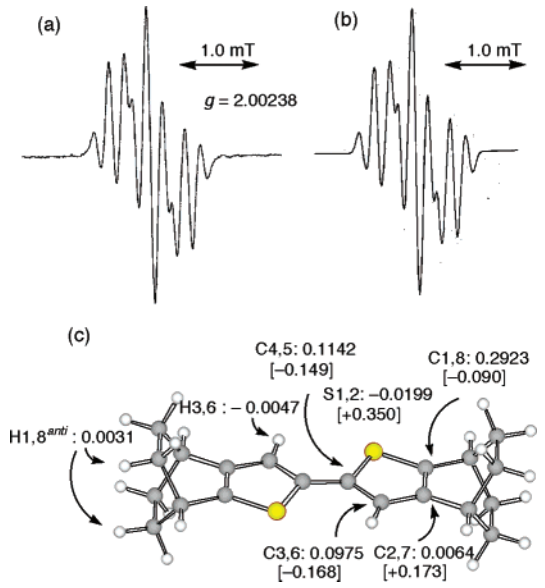


***Figure 2.*** (a) ESR spectrum of **1**(2T)$^{\bullet+}SbF_6^-$ in $CH_2Cl_2$ and (b) simulated spectrum using the calculated coupling constant for H1,8$^{anti}$ (0.19 mT, 4H) and H3,6 (−0.29 mT, 2H) obtained from the optimized structure of **1**(2T)$^{\bullet+}$ at the UB3LYP/6-31G(d) level shown in (c), in which the spin densities are shown together with the Mulliken charges in square brackets.

***Chart 1***

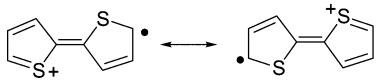

provides the first precise assessment of the degree of quinodal character based on the experimentally determined structure.

**(b) Terthiophene 1(3T).** As described above, the terthiophene radical cation salt **1**(3T)$^{\bullet+}SbF_6^-$ was prepared as air-stable dark purple crystals, and its molecular structure was also determined by X-ray crystallography. In this case, a statistical disorder was involved in the terminal thiophene rings, similar to the X-ray structure of neutral **1**(3T),[21] and the dominant form was found to be a transoid,transoid (*t*,*t*) conformer, as shown in Figure 3a. Although the DFT calculation (B3LYP/6-31G(d)) has predicted a completely planar $\pi$-system with the *t*,*t* conformation as the global energy-minimized structure for **1**(3T)$^{\bullet+}$, the observed structure was somewhat twisted, with inter-ring torsion angles of C3−C4−C5−C6 = −155.5(8)° and C7−C8−C9−C10 = −149.4(8)°. The degree of twisting in **1**(3T)$^{\bullet+}$ was smaller than that of neutral **1**(3T) (C3−C4−C5−C6, −149.7(3)°; C7−C8−C9−C10, 34.4(3)°), and the difference from the calculated structure might be ascribed to the crystal packing force.

In the crystal packing diagram shown in Figure 3b, the molecules of radical cation **1**(3T)$^{\bullet+}$ are arranged in a face-to-face fashion but slipped by nearly one thiophene unit. Due to the twisting of terminal thiophene rings, the intermolecular distance between a sulfur atom in the terminal thiophene unit and an $sp^2$ carbon in the central unit becomes relatively short (3.58 Å), yet the distance is slightly longer than the sum of the van der Waals radii of sulfur and carbon atoms (3.55 Å). As to the change in bond lengths upon one-electron oxidation of **1**(3T),

(27) (a) Keszthelyi, T.; Grage, M. M.-L.; Offersgaard, J. F.; Wilbrandt, R.; Svendsen, C.; Mortensen, O. S.; Pedersen, J. K.; Jensen, H. A. J. *J. Phys. Chem. A* **2000**, *104*, 2808. (b) Grage, M. M.-L.; Keszthelyi, T.; Offersgaard, J. F.; Wilbrandt, R. *Chem. Phys. Lett.* **1998**, *282*, 171 and references therein.

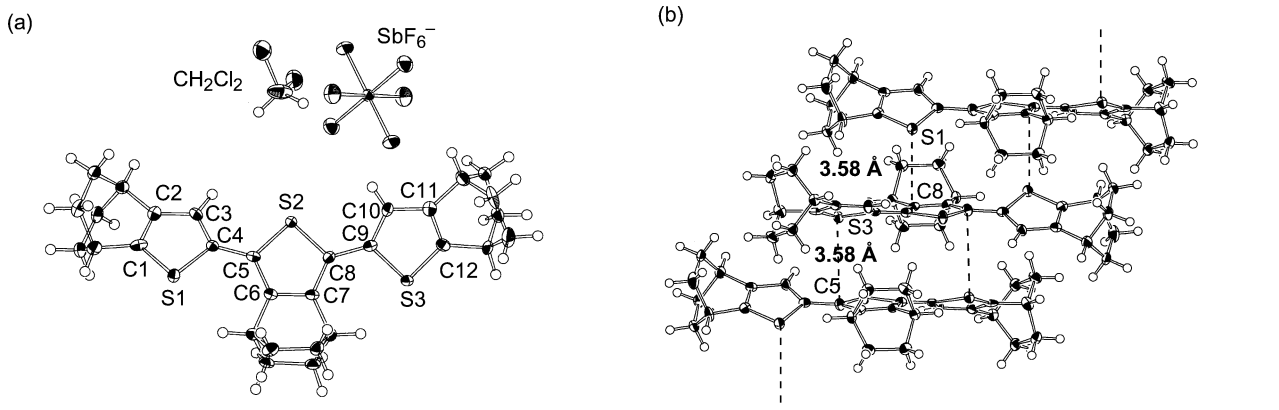


***Figure 3.*** (a) ORTEP drawing of **1**(3T)$^{\bullet+}SbF_6^-$. Thermal ellipsoids are drawn at the 50% probability level. Selected bond lengths (Å) and angles (deg): S1−C1, 1.697(6); C1−C2, 1.394(9); C2−C3, 1.389(11); C3−C4, 1.390(11); C4−S1, 1.761(6); C4−C5, 1.421(9); C5−C6, 1.424(9); C6−C7, 1.389(9); C7−C8, 1.418(9); C8−S2, 1.747(6); S2−C5, 1.751(6); C8−C9, 1.436(9); C9−S3, 1.755(6); C9−C10, 1.389(12); C10−C11, 1.411(11); C11−C12, 1.372-(10); C12−S3, 1.706(6); C1−S1−C4, 90.3(3); S1−C1−C2, 114.9(5); C1−C2−C3, 109.7(7); C2−C3−C4, 115.1(8); C3−C4−S1, 109.9(5); C5−S2−C8, 92.7(3); S2−C5−C6, 109.7(5); C5−C6−C7, 113.7(5); C6−C7−C8, 113.5(5); C7−C8−S2, 110.2(5); C9−S3−C12, 89.7(3); S3−C9−C10, 110.8(6); C9−C10−C11, 114.0(9); C10−C11−C12, 109.8(7); C11−C12−S3, 115.6(5); C3−C4−C5−C6, −155.5(8); C7−C8−C9−C10, −149.4(8). (b) Crystal packing drawing; the $SbF_6^-$ ions and $CH_2Cl_2$ are omitted for clarity.

a tendency similar to that observed in **1**(2T) was also demonstrated, as exemplified by the alteration of the inter-ring bond (C4−C5, 1.452(2) Å ($n_{C-C}$ = 1.27) → 1.421(9) Å ($n_{C-C}$ = 1.41)), the terminal C−S bond (C1−S1, 1.726(2) Å ($n_{C-S}$ = 1.47) → 1.697(6) Å ($n_{C-S}$ = 1.59)), and the terminal C−C bonds (C1−C2, 1.355(2) Å ($n_{C-C}$ =1.76) → 1.394(9) Å ($n_{C-C}$ =1.54); C2−C3, 1.425(4) Å ($n_{C-C}$ =1.39) → 1.389(11) Å ($n_{C-C}$ =1.57)). The extent of the bond-length change, however, is apparently smaller for the one-electron oxidation of **1**(3T) than for **1**(2T). In contrast to the bond equalization observed for C(α)−C(*β*) and C(*β*)−C(*β*′) in the terminal rings of **1**(3T)$^{\bullet+}$, the bond length of C(α)−C(*β*) is appreciably (>0.03 Å) longer than C(*β*)−C(*β*′) in the central ring, suggesting stronger quinoidal character in this ring.

The ESR spectrum of **1**(3T)$^{\bullet+}SbF_6^-$ in $CH_2Cl_2$ ($1.0 \times 10^{-5}$ M) was also recorded at room temperature. As shown in Figure 4a, a rather broad signal with unresolved hyperfine couplings was observed. The optimized structure of **1**(3T)$^{\bullet+}$ at the UB3LYP/6-31G(d) level (Figure 4c) showed induced spin at H1,12$^{anti}$ ($a_H$ = 0.13 mT) and at H3,10 (−0.300 mT), as observed in **1**(2T)$^{\bullet+}$. The simulated ESR spectrum using these calculated coupling constants is shown in Figure 4b. Although the general spectral pattern is similar, the experimental spectrum is less smooth, possibly due to the small coupling with more hydrogen atoms.

Considering the calculated positive charge mostly on sulfur atoms (S1, +0.325; S2, +0.317) and the spin density mostly distributed on C1, C3, and C5 (C1, 0.2084; C3, 0.1140; C5, 0.1611), quinoidal structures (Chart 2a) as well as semiquinoidal structures (Chart 2b) would be contributing as the important canonical structures for the resonance of **1**(3T)$^{\bullet+}$. The generally smaller degree of change in bond lengths upon oxidation of **1**(3T) than that of **1**(2T) appears to indicate the important contribution of the structures in Chart 2b. Thus, the purely quinoidal character in each thiophene ring of **1**(3T)$^{\bullet+}$ is less significant than that of **1**(2T)$^{\bullet+}$.

**Electronic Spectra of Radical Cations of Bithiophene 1(2T) and Terthiophene 1(3T).** The electronic spectra of solutions of **1**(2T)$^{\bullet+}SbF_6^-$ and **1**(3T)$^{\bullet+}SbF_6^-$ in $CH_2Cl_2$ at room temperature exhibited absorption maxima at 694 and 458 nm (1.78 and 2.71 eV) for **1**(2T)$^{\bullet+}$ and at 920 and 586 nm (1.35 and 2.12 eV) for **1**(3T)$^{\bullet+}$ (Figure 5). These absorptions are bathochromically shifted as compared with those of the radical cations of unsubstituted bithiophene (2.10 and 2.92 eV)[27a] and terthiophene (1.46 and 2.25 eV).[28] This is most probably ascribed to the hyperconjugative interaction of the positively charged *π*-systems with *σ*-bonds in the BCO frameworks, as has previously been observed.[23e]

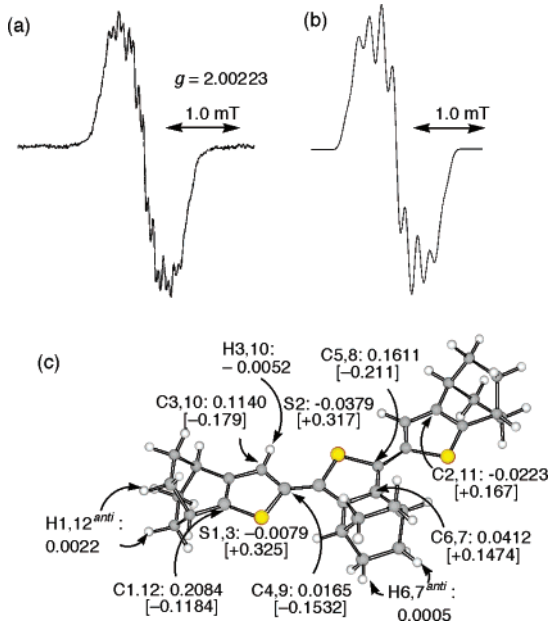


***Figure 4.*** (a) ESR spectrum of **1**(3T)$^{\bullet+}SbF_6^-$ in $CH_2Cl_2$, and (b) simulated spectrum using the calculated coupling constant for H1,12$^{anti}$ (0.13 mT, 4H) and H3,10 (−0.30 mT, 2H) obtained from the optimized structure of **1**(3T)$^{\bullet+}$ at the UB3LYP/6-31G(d) level shown in (c), in which the spin densities are shown together with the Mulliken charges in square brackets.

For oligothiophene radical cations stabilized with substituents at the α-positions of both ends, reversible spectral change supposedly corresponding to the formation of *π*-dimers has been observed in the electronic and/or ESR spectra at low temperatures.[4−9] In the present study, however, variable-temperature electronic−spectral measurements of **1**(2T)$^{\bullet+}SbF_6^-$ and

(28) Wintgens, V.; Valat, P.; Garnier, F. *J. Phys. Chem.* **1994**, *98*, 228.

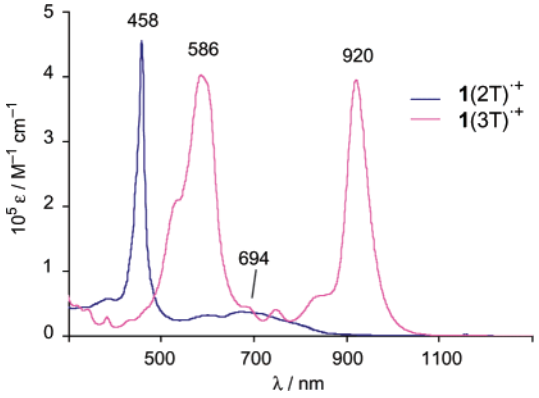


***Figure 5.*** Electronic absorption spectra of **1**(2T)$^{\bullet+}$$SbF_6^-$ and **1**(3T)$^{\bullet+}$$SbF_6^-$ at room temperature in $CH_2Cl_2$ at the concentrations of $1.86 \times 10^{-5}$ and $2.24 \times 10^{-5}$ M, respectively.

***Chart 2***

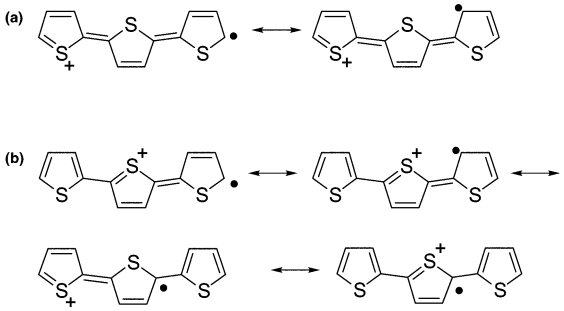


**1**(3T)$^{\bullet+}$$SbF_6^-$ in $CH_2Cl_2$ exhibited essentially no change in both spectral pattern and absorption intensity when the solution was cooled to 180 K, even at relatively high concentrations ($1.36 \times 10^{-3}$ and $1.81 \times 10^{-3}$ M, respectively), as shown in Figure 6. Also, the ESR spectra of both of these solutions exhibited no apparent decrease in intensity in the temperature range of 235−300 K. These results clearly indicate that $\pi$- or $\sigma$-dimer formation is effectively inhibited for **1**(2T)$^{\bullet+}$ and **1**(3T)$^{\bullet+}$ due to the presence of rigid and bulky BCO units.

In the bithiophene radical cation **1**(2T)$^{\bullet+}$, the central part of the $\pi$-system is not sterically protected, and the interchain interaction at this central position could have given rise to the "spinless" state, as observed in the terthiophene radical cation with bulky phenyldimethylsilyl substituents attached only to both ends.[5] Nevertheless, the formation of such a "spinless" state was proved to be inhibited, as shown by the packing structure in the solid state (Figure 1b) and by the variable-temperature UV−vis−NIR measurements in solution (Figure 6), as described above. Therefore, in the case of bithiophene radical cation, not a simple control of the $\pi$-stacking mode but a steric protection of the terminal α-positions bearing the highest spin density (Figure 2c) is apparently important to inhibit the formation of the "spinless" dimer. As an example with no such a steric protection, the radical cation of 5,5′-diphenyl-3,3′,4,4′-tetramethoxybipyrrole, which was shown to be stacked in a face-to-face fashion in the solid state, with the center-to-center distance of five-membered rings being 3.44 Å, was found to give a $\sigma$-dimer in solution.[14]

For the terthiophene radical cation, spin is distributed not only on the α-positions at both terminals but on the α-positions of the central thiophene unit, as has been shown by the calculated structure of **1**(3T)$^{\bullet+}$ (Figure 4c), and the interchain interaction

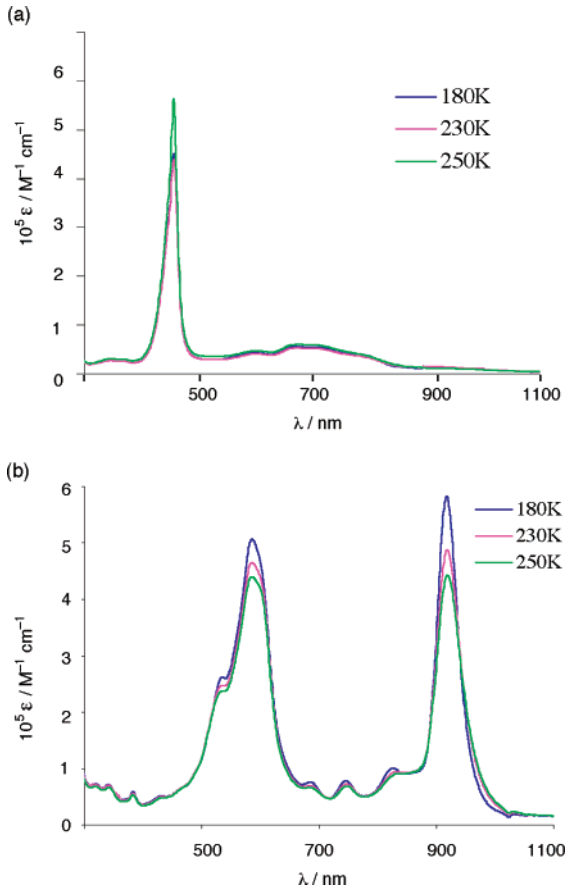


***Figure 6.*** Temperature-dependent UV−vis−NIR spectra of (a) **1**(2T)$^{\bullet+}$$SbF_6^-$ and (b) **1**(3T)$^{\bullet+}$$SbF_6^-$ in $CH_2Cl_2$ at the concentrations of $1.36 \times 10^{-3}$ and $1.81 \times 10^{-3}$ M, respectively.

at these central positions can lead to the spinless state, even when bulky substituents are attached to both ends.[5] On the other hand, even though the intermolecular distance between an $sp^2$ carbon and sulfur atoms (3.58 Å) is close to the sum of the van der Waals radii of these atoms (3.55 Å) in the crystal structure of **1**(3T)$^{\bullet+}$ (Figure 3b), formation of the spinless dimer was not observed at all in solution, probably due to the very small spin distribution on the sulfur atom (−0.0079; Figure 4c). Thus, a barrier-free approach of carbons with high spin density is important for the formation of a spinless dimer, but the involvement of the $\sigma$-bond character in the spinless dimer in the solid state still remains elusive.

**NMR Observation of Dications of Bithiophene 1(2T) and Terthiophene 1(3T).** Following our success in isolating the radical cation salts of bithiophene **1**(2T) and terthiophene **1**(3T), we attempted their two-electron oxidation by the use of an excess amount (20−30 equiv) of $SbF_5$ in $CD_2Cl_2$ at −78 °C in a vacuum-sealed tube. The red and dark blue solutions resulting from **1**(2T) and **1**(3T), respectively, exhibited $^1H$ and $^{13}C$ NMR signals at relatively lower field, as shown in Figures 7 and 8, respectively. By comparison with the calculated NMR chemical shifts (GIAO/HF/6-31+G(d)//B3LYP/6-31G(d); for $^1H$ NMR see Table 1, and for $^{13}C$ NMR see Supporting Information), the observed signals were unambiguously assigned to **1**(2T)$^{2+}$ and **1**(3T)$^{2+}$ (Scheme 2).

In the $^1H$ NMR spectrum of **1**(2T)$^{2+}$, two signals corresponding to the protons (C($\beta$)H) directly attached to the thiophene rings (C3) were observed at 8.48 and 8.26 ppm, with an in-

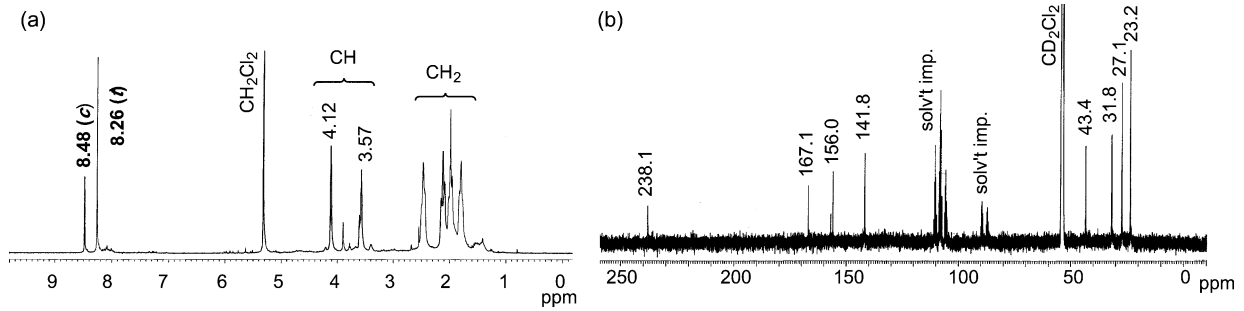


***Figure 7.*** (a) $^1$H (400 MHz) and (b) $^{13}$C (100 MHz) NMR spectra of **1**(2T)$^{2+}$ (*t*:*c* = 2.3:1) in $CD_2Cl_2$ at −40 °C.

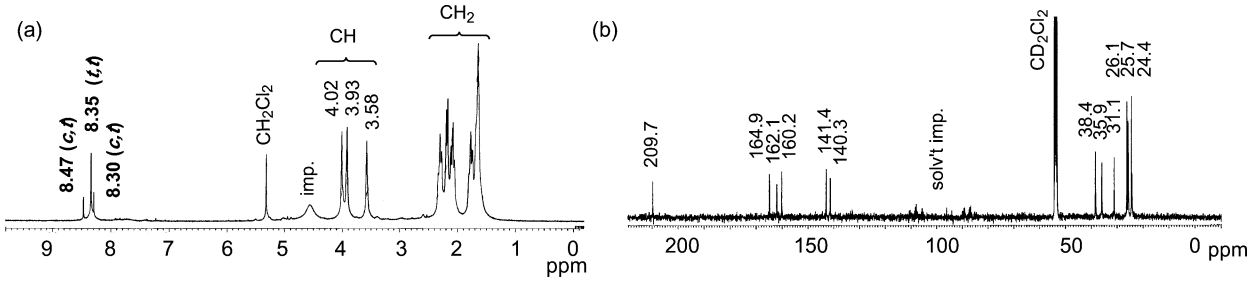


***Figure 8.*** (a) $^1$H (400 MHz) and (b) $^{13}$C (100 MHz) NMR spectra of **1**(3T)$^{2+}$ (*t*,*t*:*c*,*t* = 3.5:1) in $CD_2Cl_2$ at 23 °C.

***Table 1.*** Observed[a] and Calculated[b] $^1$H NMR Chemical Shifts ($\delta$) for **1**(2T)$^{2+}$ and **1**(3T)$^{2+}$

| | | | C($\beta$)H | | CH (BCO) | | | CH$_2$ (BCO) | | | | |
|---|---|---|---|---|---|---|---|---|---|---|---|---|
| **1**(2T)$^{2+}$ | obsd | 8.48[c] | | 8.26[d] | 4.11 | 3.57 | | 2.47 (4H) | 2.12 (4H) | 1.99 (4H) | | 1.80 (4H) |
| | calcd (*t*)[e] | | 8.33 | | 3.89 | 3.41 | | 2.82[f] | 2.51[f] | 1.82[g] | | 1.70[g] |
| | calcd (*c*)[h] | | 8.57 | | 3.87 | 3.43 | | 2.81[f] | 2.51[f] | 1.81[g] | | 1.72[g] |
| | | | C($\beta$)H | | CH (BCO) | | | | CH$_2$ (BCO) | | | |
| **1**(3T)$^{2+}$ | obsd | 8.47[i] | 8.35[j] | 8.30[i] | 4.02 | 3.93 | 3.58 | 2.24 (4H) | 2.12 (4H) | 2.03 (4H) | 1.70 (4H) | 1.59 (8H) |
| | calcd (*t*,*t*)[k] | | 8.70 | | 3.63 | 3.32 | 3.30 | 2.48[f] | 2.30[f] | 2.23[f] | 1.61[g] 1.56[g] | 1.48[g] |
| | calcd (*c*,*t*)[l] | 8.88 | | 8.68 | 3.63 | 3.33 | 3.27 | 2.49[f] | 2.29[f] | 2.25[f] | 1.62[g] 1.59[g] | 1.56[g] |
| | | | | | 3.60 | 3.28 | 3.24 | 2.46[f] | 2.27[f] | 2.26[f] | 1.59[g] 1.55[g] | 1.53[g] |

[a] In $CD_2Cl_2$. [b] At the GIAO/HF/6-31+G(d)//B3LYP/6-31G(d) level. [c] Assigned to the signal for the cisoid conformer. [d] Assigned to the signal for the transoid conformer. [e] Transoid conformer. [f] *Anti* proton. [g] *Syn* proton. [h] Cisoid conformer. [i] Assigned to the signal for the cisoid,transoid conformer. [j] Assigned to the signal for the transoid,transoid conformer. [k] Transoid,transoid conformer. [l] Cisoid,transoid conformer.

***Scheme 2***

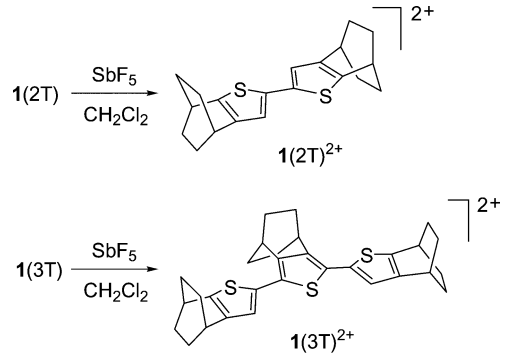


***Chart 3***

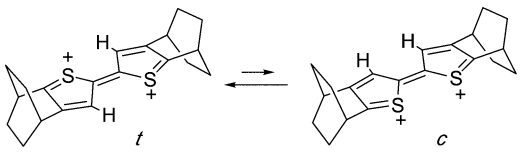


tegrated ratio of 1:2.3. These signals are assigned to the protons of cisoid (*c*) and transoid (*t*) conformers (Chart 3), respectively, on the basis of comparison with calculated chemical shifts (*c*, 8.57 ppm; *t*, 8.33 ppm). Apparently, the exchange between the transoid and cisoid conformers must be quite slow on the NMR time scale. As to the calculated $^1$H NMR chemical shifts for other protons, the differences between the two conformers are relatively small, and the signals for the two conformers, except for the C($\beta$)H protons, are likely to be overlapped in the observed NMR spectra.

Even when the solution of **1**(2T)$^{2+}$ was warmed to 20 °C, no line broadening was observed in the NMR signals for C($\beta$)H protons. Thus, the coalescence temperature ($T_c$) should be much higher than 20 °C, and the energy barrier ($\Delta G^{\ddagger}$) for the inter-ring bond rotation is estimated to be much larger than 14 kcal mol$^{-1}$. Actually, the inter-ring rotational barrier was calculated to be 27.6 kcal mol$^{-1}$ for the dication of parent bithiophene at the B3LYP/6-31G(d) level (Figure 9), the value being fairly close to the previously reported one (35.5 kcal mol$^{-1}$ at the UHF/6-31G(d) level[29]). Thus, although the rotational barrier is quite small in the case of neutral bithiophene (estimated to be 1.04 kcal mol$^{-1}$ at the MP2/6-31G(d) level[30]), it is greatly increased due to the enhanced double bond character of the inter-ring bond in the dication. According to theoretical calculations, the inter-ring bond length in **1**(2T)$^{2+}$ (1.368 Å at B3LYP/6-31G(d)) is significantly shortened, with the bond order of 1.69,[25,26] as compared with those in neutral **1**(2T) (1.449 Å),

(29) Alemán, C.; Julia, L. *J. Phys. Chem.* **1996**, *100*, 14661.
(30) Diaz-Quijada, G. A.; Weinberg, N.; Holdcroft, S.; Pinto, B. M. *J. Phys. Chem. A* **2002**, *106*, 1266.

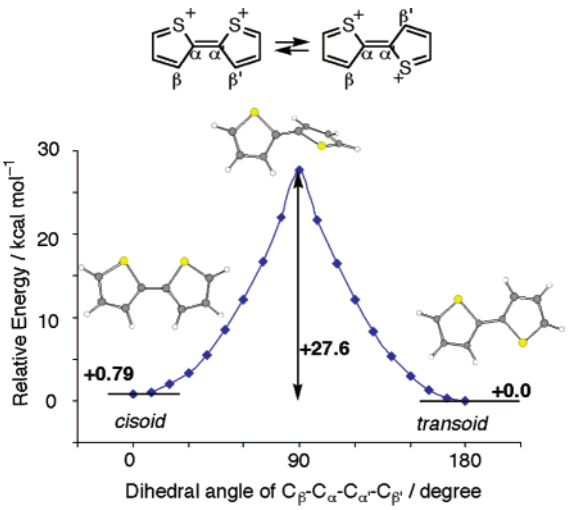


***Figure 9.*** Inter-ring torsional energy profile for the 2,2′-bithiophene dication at the B3LYP/6-31G(d) level.

with the bond order of 1.28, and with radical cation **1**(2T)$^{\bullet+}$ (1.405 Å), with the bond order of 1.49.

On the basis of the equilibrium constant obtained from the integrated ratio of the C($\beta$)H signals of the two conformers (*t*:*c* = 2.3:1), the free energy difference for the equilibrium shown in Chart 3 ($\Delta G°(c-t)$) is calculated to be 0.38 kcal mol$^{-1}$ at −40 °C. This is in fair agreement with the calculated result that the *t* conformer is more stable than the *c* conformer by 0.79 kcal mol$^{-1}$ in **1**(2T)$^{2+}$.

On the other hand, the observed NMR signals for C($\beta$)H protons of **1**(3T)$^{2+}$ can be explained as follows. According to the results of theoretical calculations for **1**(3T)$^{2+}$ at the B3LYP/6-31G(d) level, the *t*,*t* conformer, with a completely planarized $\pi$-system, was shown to be the global minimum and the *c*,*t* and *c*,*c* conformers were calculated to be 1.5 and 3.0 kcal mol$^{-1}$ less stable, respectively. Thus, the population of the *c*,*c* conformer should be negligibly small in the equilibrium among these three conformers, and the observed one strong signal at 8.35 ppm and two weak signals at 8.47 and 8.30 ppm can be assigned to the C($\beta$)H protons of the *t*,*t* and *c*,*t* conformers, respectively. Although the calculated values for the $^1$H NMR chemical shifts for C($\beta$)H are 0.35 to 0.4 ppm more downfield shifted (Table 1), they qualitatively support the present assignments (the signal at 8.35 ppm for the *t*,*t* conformer and those at 8.47 and 8.30 ppm for the *c*,*t* conformer). The $\Delta G°$ value, estimated from the distribution of *t*,*t* and *c*,*t* conformers determined by the integrated ratio of 3.5:1 for the corresponding NMR signals, is 0.74 kcal mol$^{-1}$ at 23 °C, and this can be compared with the calculated energy difference between these two conformers (1.5 kcal mol$^{-1}$), in favor of the *t*,*t* conformer. Again, the rotational barrier should be much higher than 14 kcal mol$^{-1}$ because the coalescence temperature should be much higher than 23 °C in NMR. Actually, the calculated rotational barrier between *t*,*t* and *c*,*t* conformers is 22.9 kcal mol$^{-1}$ for the dication of the unsubstituted terthiophene.

The results of the calculated bond lengths shown in Table 2 indicate that the tendency in bond alternations of C(sp$^2$)−C(sp$^2$) bonds in dications **1**(2T)$^{2+}$ and **1**(3T)$^{2+}$ is totally reversed from that of neutral molecules due to the formation of the quinoidal structures depicted in Charts 3 and 4. It is noteworthy that the bond orders[25,26] of S−C1 (**1**(2T), 1.43; **1**(2T)$^{\bullet+}$, 1.50; **1**(2T)$^{2+}$, 1.58; **1**(3T), 1.44; **1**(3T)$^{\bullet+}$, 1.49; **1**(3T)$^{2+}$, 1.55), C2−C3 (**1**(2T), 1.40; **1**(2T)$^{\bullet+}$, 1.56; **1**(2T)$^{2+}$, 1.70; **1**(3T), 1.41; **1**(3T)$^{\bullet+}$, 1.53; **1**(3T)$^{2+}$, 1.64), and inter-ring bonds C4−C5 (**1**(2T), 1.28; **1**(2T)$^{\bullet+}$, 1.49; **1**(2T)$^{2+}$, 1.69; **1**(3T), 1.27; **1**(3T)$^{\bullet+}$, 1.43; **1**(3T)$^{2+}$, 1.58) become greater as the net positive charge per one thiophene ring increases.

***Chart 4***

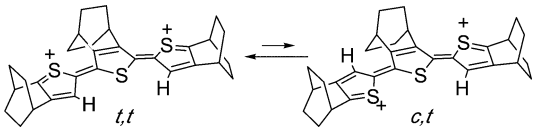


**Preparation and Properties of Dication Salts of Quaterthiophene 1(4T) and Sexithiophene 1(6T).** The previous electrochemical study on thiophene oligomers **1**(2T) to **1**(6T)[21] indicated that the first and second one-electron oxidations become quite facile according to the elongation of the oligothiophene main chain. The first oxidation potential for both **1**(4T) and **1**(6T) reached a value as low as +0.19 V vs Fc/Fc$^+$, while the second oxidation potentials for **1**(4T) and **1**(6T) were lowered to +0.46 and +0.28 V, respectively. Apparently reflecting such lowering in oxidation potential, the chemical oxidation of quaterthiophene **1**(4T) with 1 equiv of NO$^+$SbF$_6^-$ afforded not the radical cation but the dication **1**(4T)$^{2+}$. Thus, when the reaction was conducted in $CH_2Cl_2$ at room temperature under vacuum, giving a dark green solution, and hexane was slowly diffused into this solution under argon over 4 days, dark blue crystals with a gold luster were obtained. The X-ray structural analysis revealed that this crystal was the dication salt **1**(4T)$^{2+}$(SbF$_6^-$)$_2$ (Scheme 3, Figure 10). The yield of **1**(4T)$^{2+}$2SbF$_6^-$ was 26% under the above conditions and 46% when 2 equiv of NO$^+$SbF$_6^-$ was used. The dication salt was remarkably stable and showed no decomposition upon standing under air for more than 1 month.

In the X-ray structure of **1**(4T)$^{2+}$(SbF$_6^-$)$_2$, two SbF$_6^-$ counteranions are located above and below the quaterthiophene dication moiety, as shown in Figure 10a, and no intermolecular contact between the $\pi$-systems was observed due to the steric hindrance of the bicyclic frameworks, as shown in Figure 10c. The quaterthiophene $\pi$-system has all *anti* and completely planar conformation (Figure 10b), with the dihedral angles C3−C4−C5−C6 = −179.6(6)° and C7−C8−C9−C10 = 180.0°. The optimized structure of **1**(4T)$^{2+}$ (B3LYP/6-31G(d)), having a singlet electronic state, was also calculated to be planar, as in the case of **1**(2T)$^{\bullet+}$ and **1**(3T)$^{\bullet+}$.

Similarly to the case of radical cation **1**(2T)$^{\bullet+}$, this planarization in dication **1**(4T)$^{2+}$ is accompanied by considerable shortening of the inter-ring bonds (C4−C5, 1.383(7) Å, with the bond order of 1.58,[25,26] and C8−C9, 1.390(11) Å with the bond order of 1.56[25,26]) in comparison with the parent neutral quaterthiophene (**4**) (1.435(8) and 1.424(12) Å, respectively).[31] These inter-ring bond lengths and their bond orders of dication **1**(4T)$^{2+}$ are comparable to those of radical cation **1**(2T)$^{\bullet+}$ (1.398(8) Å (bond order, 1.52)) and apparently shorter and higher, respectively, than those of radical cation **1**(3T)$^{\bullet+}$ (1.421(9) Å (bond order, 1.41) and 1.436(9) Å (bond order, 1.34)). In the central thiophene rings of **1**(4T)$^{2+}$, a change in bond alternation

(31) Siegrist, T.; Kloc, C.; Laudise, R. A.; Katz, H. E.; Haddon, R. C. *Adv. Mater.* **1998**, *10*, 379.

***Table 2.*** Calculated[a] Bond Lengths (Å) in $\pi$-Conjugated Systems of **1**(2T), **1**(2T)$^{\bullet+}$, **1**(2T)$^{2+}$, **1**(3T), **1**(3T)$^{\bullet+}$, and **1**(3T)$^{2+}$

| | S1–C1 | C1–C2 | C2–C3 | C3–C4 | C4–S1 | C4–C5 | S2–C5 | C5–C6 | C6–C7 |
|---|---|---|---|---|---|---|---|---|---|
| **1**(2T) | 1.735 | 1.371 | 1.422 | 1.381 | 1.767 | 1.449 | | | |
| **1**(2T)$^{\bullet+}$ | 1.719 | 1.406 | 1.390 | 1.414 | 1.779 | 1.405 | | | |
| **1**(2T)$^{2+}$ | 1.700 | 1.450 | 1.366 | 1.445 | 1.807 | 1.368 | | | |
| **1**(3T) | 1.733 | 1.371 | 1.421 | 1.382 | 1.768 | 1.452 | 1.763 | 1.378 | 1.430 |
| **1**(3T)$^{\bullet+}$ | 1.720 | 1.393 | 1.397 | 1.408 | 1.776 | 1.417 | 1.768 | 1.412 | 1.403 |
| **1**(3T)$^{2+}$ | 1.705 | 1.423 | 1.376 | 1.387 | 1.791 | 1.387 | 1.774 | 1.442 | 1.383 |

[a] At the B3LYP/6-31G(d) level.

***Scheme 3***

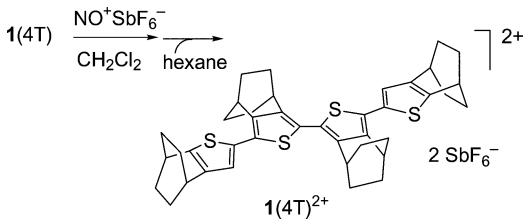


pattern similar to that observed in **1**(2T)$^{\bullet+}$—that is, a reversal in the single and double bond character in $\pi$-bonds—was apparent. Thus, bonds C5−C6 (1.408(8) Å (bond order, 1.47)) and C7−C8 (1.417(8) Å (bond order, 1.43)) are elongated compared with the same bonds in neutral quaterthiophene **4** (1.395(8) and 1.343(8) Å, respectively), and the bond C6−C7 (1.358(7) (bond order, 1.74)) is much shorter than that in **4** (1.431(8) Å). Also in the terminal thiophene rings, similar bond-length changes were observed: C1−S1 (1.668(6) Å (bond order, 1.72)) and C2−C3 bonds (1.385(8) Å (bond order, 1.59)) are shortened compared with the same bonds in **4** (1.737(7) and 1.427(9) Å, respectively), and the C1−C2 bond (1.372(8) Å (bond order, 1.66)) is longer than that in **4** (1.320(11) Å). However, the bond lengths of C1−C2, C2−C3, and C3−C4 (1.388(8) Å (bond order, 1.57)) are quite similar to each other, in contrast to the bond-length change observed in the central thiophene rings. This suggests that the quinoidal character is more prominent in the central units, possibly due to the contribution of resonance structure with neutral thiophene ring-(s) at the terminal units. In addition, the calculated charge distribution in dication **1**(4T)$^{2+}$ indicated that the difference in positive charge between S1 (+0.381) and S2 (+0.358) is smaller than that in **1**(3T)$^{2+}$ (S1, +0.416; S2, +0.374). Thus, the electronic structure of the quaterthiophene dication can be depicted as the resonance involving quinoidal structures shown in Chart 5.

In exactly the same way as above, the oxidation of sexithiophene **1**(6T) with 1 equiv of $NO^+SbF_6^-$ in $CH_2Cl_2$ at room temperature, followed by slow diffusion of hexane, afforded dark green crystals with a gold luster. The X-ray structural analysis revealed again that the crystal was not the radical cation salt but the dication salt **1**(6T)$^{2+}$($SbF_6^-$)$_2$ (Scheme 4, Figures 11 and 12). The yield of **1**(6T)$^{2+}$2$SbF_6^-$ was 46% under the above conditions and 73% when 2 equiv of $NO^+SbF_6^-$ was used. The salt **1**(6T)$^{2+}$($SbF_6^-$)$_2$ was as stable as **1**(4T)$^{2+}$($SbF_6^-$)$_2$.

The X-ray structure of **1**(6T)$^{2+}$($SbF_6^-$)$_2$ demonstrated that the sexithiophene dication moiety has also an all-*anti* conformation, as shown in Figure 11. In the crystal packing structure (Figure 12), two molecules are paired in a face-to-face fashion and slipped by one thiophene unit (Figure 12a). However, the intermolecular distances between the sp$^2$ carbons (3.86−4.56 Å) are much longer than the sum of the van der Waals radii of

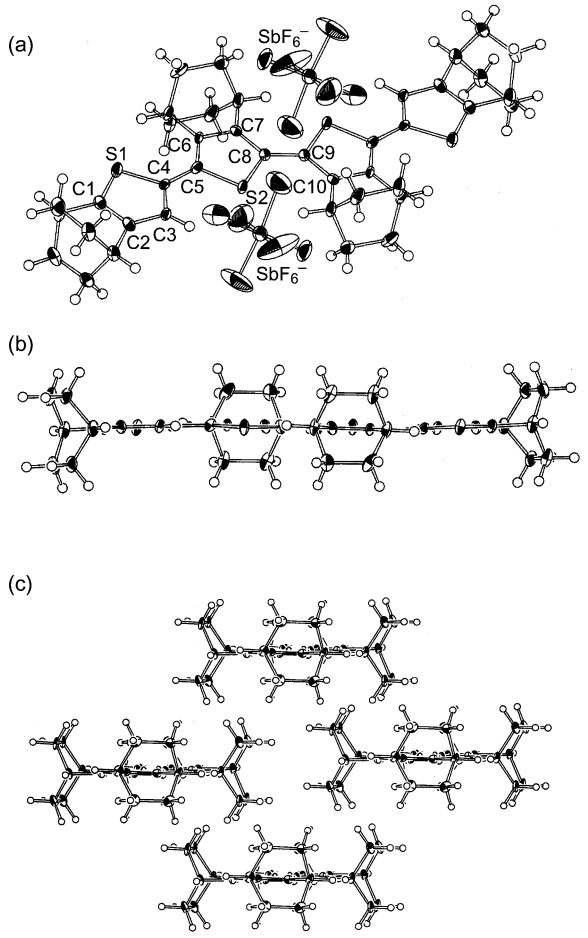


***Figure 10.*** (a) ORTEP drawing of **1**(4T)$^{2+}$($SbF_6^-$)$_2$. Thermal ellipsoids are drawn at the 50% probability level. Selected bond lengths (Å) and angles (deg): S1−C1, 1.668(6); C1−C2, 1.372(8); C2−C3, 1.385(8); C3−C4, 1.388(8); C4−S1, 1.743(6); C4−C5, 1.383(7); C5−C6, 1.408(8); C6−C7, 1.358(7); C7−C8, 1.417(8); C8−S2, 1.733(6); S2−C5, 1.730(6); C8−C9, 1.390(11); C1−S1−C4, 90.5(3); S1−C1−C2, 114.7(5); C1−C2−C3, 111.3-(5); C2−C3−C4, 112.8(5); C3−C4−S1, 110.7(4); C5−S2−C8, 92.3(3); S2−C5−C6, 109.8(4); C5−C6−C7, 114.6(5); C6−C7−C8, 112.9(5); C7−C8−S2, 110.3(4); C3−C4−C5−C6, −179.6(6); C7−C8−C9−C10, 180.0. (b) Side view and (c) crystal packing drawing. The counter anions $SbF_6^-$ are omitted for clarity in (b) and (c).

***Chart 5***

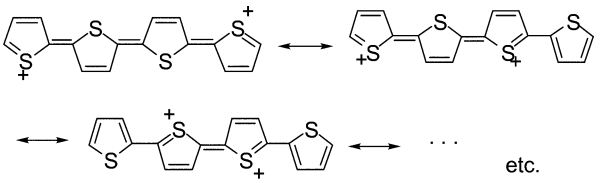


sp$^2$ carbon atoms (3.40 Å), indicating that no intermolecular $\pi-\pi$ interaction is present between the cationic $\pi$-systems in the solid state. The $\pi$-system in **1**(6T)$^{2+}$ is essentially planar

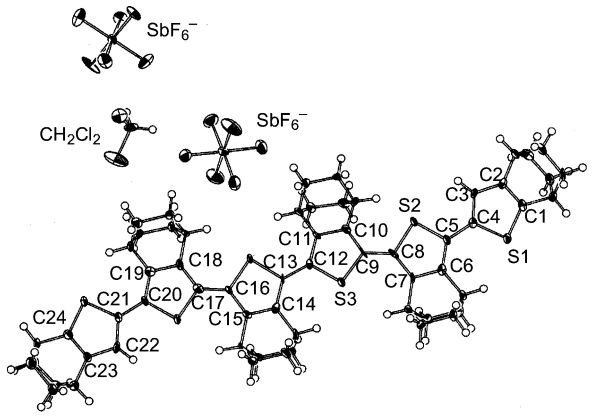


***Figure 11.*** (a) ORTEP drawing of **1**(6T)$^{2+}$($SbF_6^-$)$_2$($CH_2Cl_2$). Thermal ellipsoids are drawn at the 50% probability level. Selected bond lengths (Å) and angles (deg): S1−C1, 1.717(11); C1−C2, 1.370(14); C2−C3, 1.419(14); C3−C4, 1.393(14); C4−S1, 1.775(10); C4−C5, 1.442(14); C5−C6, 1.411(14); C6−C7, 1.404(13); C7−C8, 1.417(14); C8−S2, 1.767(10); S2−C5, 1.747(10); C8−C9, 1.418(14); C9−C10, 1.439(14); C10−C11, 1.402(14); C11−C12, 1.438(14); C9−S3, 1.740(10); S3−C12, 1.769(10); C12−C13, 1.410(13); C3−C4−C5−C6, 178.0(11); C7−C8−C9−C10, 158.8(11); C11−C12−C13−C14, 161.6(8); C15−C16−C17−C18, −173.2-(11); C19−C20−C21−C22, 169.9(11).

***Scheme 4***

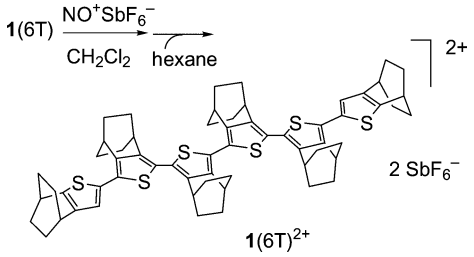


but exhibits a slightly twisted conformation with the following inter-ring torsion angles: C3−C4−C5−C6, 178.0(11)°; C7−C8−C9−C10, 158.8(11)°; C11−C12−C13−C14, 161.6(11)°; C15−C16−C17−C18, −173.2(11)°; and C19−C20−C21−C22, 169.9(11)°. In analogy to the result of the calculated structure of **1**(3T)$^{\bullet+}$, in which the net charge per one thiophene unit is the same as that in **1**(6T)$^{2+}$, the conformation of **1**(6T)$^{2+}$ is expected to be planar. Thus, the observed distortion between the thiophene rings should be ascribed to the crystal packing forces.[32]

Concerning the C(sp$^2$)−C(sp$^2$) bond length in the $\pi$-conjugated system in dication **1**(6T)$^{2+}$, a similar phenomenon is observed, although the esd values are relatively large. That is, C($\alpha$)−C($\beta$) bonds in the terminal rings are shorter than the C($\beta$)−C($\beta'$) bond, while they become slightly longer than the C($\beta$)−C($\beta'$) bonds in the next rings, and this tendency is more enhanced in the central two rings. This tendency indicates that the electronic structure of the terminal rings is closer to that of neutral thiophene, while the quinoidal character becomes greater in the rings closer to the central position.

The electronic absorption spectra of dications **1**(4T)$^{2+}$ and **1**(6T)$^{2+}$ in $CH_2Cl_2$ are shown in Figure 13, together with that of **1**(3T)$^{2+}$ generated with $SbF_5$. As expected, the longest-wavelength absorption of these dications (**1**(3T)$^{2+}$, 628 nm (1.97 eV); **1**(4T)$^{2+}$, 788 nm (1.57 eV); **1**(6T)$^{2+}$, 1158 nm (1.07 eV)) undergoes a bathochromic shift with an increase in the chain length, and a linear correlation is observed between the absorption energy and inverse chain length, as shown in Figure 14. The inclination in the linear relationship in **1**($n$T)$^{2+}$ (5.40) is apparently larger than that observed for a series of neutral **1**($n$T) (1.14),[21] in which the degree of $\pi$-conjugation is lower than that of cationic species due to distortion between the thiophene rings. Such a large difference in the inclination was not observed between neutral and oxidized oligothiophenes end-capped with cyclohexene.[6b] From such a linear correlation, the

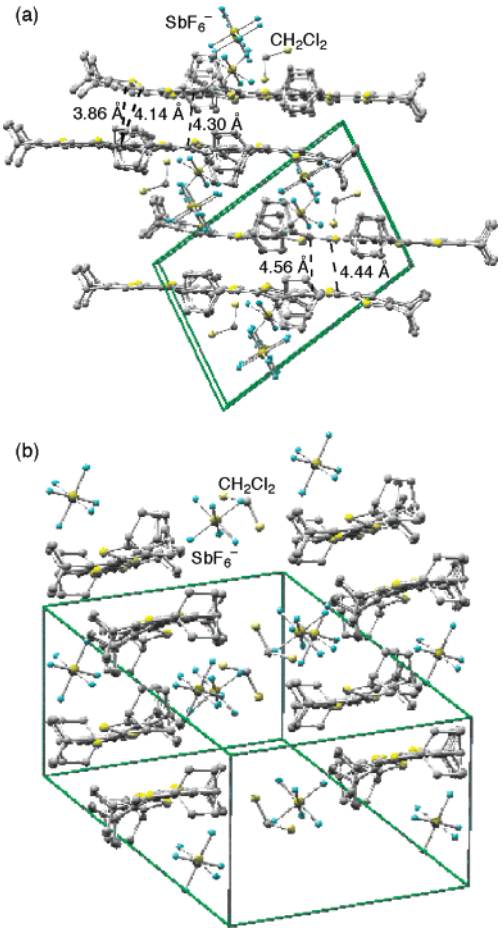


***Figure 12.*** (a) Front view and (b) side view of crystal packing drawing of **1**(6T)$^{2+}$($SbF_6^-$)$_2$($CH_2Cl_2$). The hydrogen atoms are omitted for clarity.

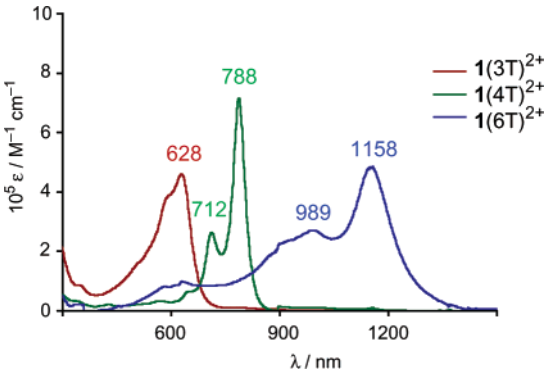


***Figure 13.*** Electronic absorption spectra of **1**(3T)$^{2+}$ generated with $SbF_5$ and the dictation salts of **1**(4T)$^{2+}$($SbF_6^-$)$_2$ and **1**(6T)$^{2+}$($SbF_6^-$)$_2$ at room temperature in $CH_2Cl_2$ at the concentrations of 2.11 × 10$^{-4}$, 2.98 × 10$^{-5}$, and 2.59 × 10$^{-5}$ M, respectively.

(32) In any case, the energy required to twist the thiophene−thiophene bond to the observed distortion angles (2−22°) would be quite small, as judged from the energy profile of the inter-ring rotation in the bithiophene dication, as shown in Figure 9.

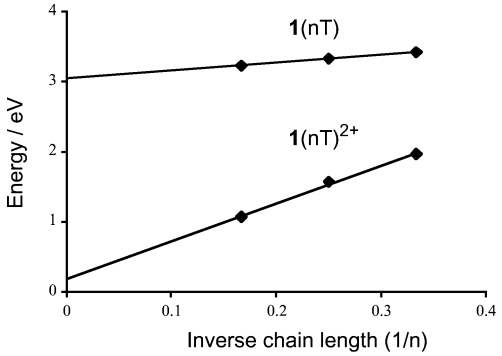


***Figure 14.*** Correlation of the longest-wavelength absorption of **1**(*n*T) and **1**(*n*T)$^{2+}$ with the inverse chain lenth (1/*n*).

degree of $\pi$-conjugation in **1**(6T)$^{2+}$ is supposed to be similar to that of **1**(4T)$^{2+}$, which was shown to be completely planar in the solid sate, and the planar conformation would be the ground-state structure of these dications in solution.

Finally, we attempted to observe $^1$H NMR spectra of dication salts **1**(4T)$^{2+}$($SbF_6^-$)$_2$ and **1**(6T)$^{2+}$($SbF_6^-$)$_2$ dissolved in $CD_3CN$. However, only very broadened spectra were observed for both dications at room temperature and even at −40 °C. The same result was obtained for the quaterthiophene dication **1**(4T)$^{2+}$ prepared in situ from **1**(4T) and $SbF_5$ in $CD_2Cl_2$. On the other hand, both of these dication salts exhibited a sharp single-line ESR signal ($g = 2.003$) in the solid sate. These results clearly indicate the presence of some paramagnetic species, which would be in equilibrium with singlet **1**(4T)$^{2+}$($SbF_6^-$)$_2$ and **1**(6T)$^{2+}$($SbF_6^-$)$_2$.[33] In a recent theoretical study on dications of a series of oligothiophenes using DFT calculations, the open-shell (two-polaron) state in the sexithiophene dication was predicted to be slightly more stable than the closed-shell (bipolaron) state by 0.18 kcal mol$^{-1}$.[34] Therefore, it is quite possible that open-shell paramagnetic species are in equilibrium with the dications **1**(4T)$^{2+}$ and **1**(6T)$^{2+}$. If this is the case, the "two-polaron state" in a single oligothiophene chain should *not* be ESR-inactive, as claimed by Janssen et al.,[8a] but ESR-active, and this suggests that the ESR inactivity of not only the radical cation but also the dication of the unprotected oligthiophene dication, with a longer chain, might be due to the formation of the interchain dimer.

## Conclusion

The radical cations and dications of a series of oligothiophenes fully surrounded by bicyclo[2.2.2]octene frameworks have been prepared, and their properties have been determined. By virtue of this structural modification, we have succeeded in the first systematic X-ray structural analysis of the radical cation salts of bi- and terthiophenes, **1**(2T)$^{\bullet+}$($SbF_6^-$) and **1**(3T)$^{\bullet+}$($SbF_6^-$), and dication salts of quater- and sexithiophenes, **1**(4T)$^{2+}$($SbF_6^-$)$_2$ and **1**(6T)$^{2+}$($SbF_6^-$)$_2$, obtained as single crystals that are stable at room temperature under air. Whereas all the previously reported oligothiophene radical cations have been reported to readily dimerize, such dimerization of **1**(2T)$^{\bullet+}$ and **1**(3T)$^{\bullet+}$ is prohibited, as shown by the crystal packing structures, and has been confirmed by low-temperature UV−vis−NIR and ESR measurements in solutions. On the basis of the packing structures and theoretical calculations of these radical cations, steric protection of carbons bearing high spin-density is considered to be important for the inhibition of the dimerization. The crystal packing structures of dication salts **1**(4T)$^{2+}$($SbF_6^-$)$_2$ and **1**(6T)$^{2+}$($SbF_6^-$)$_2$ also demonstrate effective separation of the $\pi$-systems.

On the other hand, the presence of quinoidal character in the electronic states of these cationic oligothiophenes has been demonstrated by examination of the bond lengths of the solid-state structures and the results of theoretical calculations on all of these cationic oligothiophenes, as well as by $^1$H NMR spectra of **1**(2T)$^{2+}$ and **1**(3T)$^{2+}$. The double-bond character of the inter-ring bonds due to the contribution of quinoidal resonance structure has been shown to be enhanced with the increase of the net positive charge per one thiophene ring, and this is in accord with planarization of the cationic oligothiophenes in solution. In conclusion, we have synthesized novel oligothiophenes in which the cationic $\pi$-conjugated systems are highly stabilized and are kinetically protected from dimerization without serious distortion of the planar $\pi$-system. Further elucidation of the properties of cationic oligothiophenes would be possible for longer oligomers by applying the present structural modification of BCO annelation. In addition, the steric inhibition of dimerization of the cationic $\pi$-conjugated oligomers can be considered as an important technique to clarify the intrinsic properties of unimolecular long $\pi$-conjugated system and for fabrication of "insulated molecular wires" in molecular devices. Efforts along this line are now underway in our laboratories.

## Experimental Section

**Computational Method.** All calculations were conducted using Gaussian 98 programs.[35] The geometries were optimized with the restricted Becke hybrid (B3LYP) at the 6-31G(d) level for dications, and with the unrestricted B3LYP (UB3LYP) method for radical cations. The GIAO calculations were carried out at the HF/6-31+G* level for the geometries optimized at the B3LYP/6-31G* level.

**Synthesis of 1(2T)$^{\bullet+}$$SbF_6^-$.** Bithiophene **1**(2T)[21] (19.4 mg, $5.94 \times 10^{-2}$ mmol) and $NO^+SbF_6^-$ (15.8 mg, $5.94 \times 10^{-2}$ mmol) were placed in a Pyrex glass tube connected to a vacuum line, and $CH_2Cl_2$ (1.5 mL), which had been dried over $CaH_2$ and degassed by three freeze−pump−thaw cycles, was vapor-transferred directly into the tube. The tube was disconnected under vacuum. After 10 min, when **1**(2T) and $NO^+SbF_6^-$ were completely dissolved to give a deep green-colored solution by mixing, the tube was connected to the vacuum line again, and the reaction mixture was cooled to −78 °C. Hexane (3.0 mL), which had been dried over $CaH_2$ and degassed by three freeze−pump−thaw cycles, was vapor-transferred and layered directly onto this dark green solution cooled at −78 °C, and then the tube was filled with argon. After the solution was left to stand at room temperature for 2 weeks, salt **1**(2T)$^{\bullet+}$$SbF_6^-$ (20.2 mg, 60.5%) was obtained by filtration as dark green crystals suitable for X-ray analysis: mp 236.0−240.2 °C (dec); UV−vis ($CH_2Cl_2$) $\lambda_{max}$ (log $\epsilon$) = 458 (4.68), 694 nm (3.58).

(33) To rigorously eliminate the possibility of contamination of the dication with a small amount of radical cation, the synthesis of the longer oligomer dication **1**(*n*T)$^{2+}$ ($n \geq 8$) is now under way.

(34) Gao, Y.; Liu, C.-G.; Jiang, Y.-S. *J. Phys. Chem. A* **2002**, *106*, 5380.

(35) Frisch, M. J.; Trucks, G. W.; Schlegel, H. B.; Scuseria, G. E.; Robb, M. A.; Cheeseman, J. R.; Zakrzewski, V. G.; Montgomery, J. A., Jr.; Stratmann, R. E.; Burant, J. C.; Dapprich, S.; Millam, J. M.; Daniels, A. D.; Kubin, K. N.; Strain, M. C.; Farkas, O.; Tomasi, J.; Barone, V.; Cossi, M.; Cammi, R.; Mennucci, B.; Pomelli, C.; Adamo, C.; Clifford, S.; Ochterski, J.; Petersson, G. A.; Ayala, P. Y.; Cui, Q.; Morokuma, K.; Malick, D. K.; Rabuck, A. D.; Raghavachari, K.; Foresman, J. B.; Cioslowski, J.; Ortiz, J. V.; Stefanov, B. B.; Liu, G.; Liashenko, A.; Piskorz, P.; Komaromi, I.; Gomperts, R.; Martin, R. L.; Fox, D. J.; Keith, T.; Al-Laham, M. A.; Peng, C. Y.; Nanayakkara, A.; Gonzalez, C.; Challacombe, M.; Gill, P. M.; Head-Gordon, M.; Replogle, E. S.; Pople, J. A. *Gaussian 98*, revision A.5; Gaussian, Inc.: Pittsburgh, PA, 1998.

**Synthesis of 1(3T)$^{\bullet+}$SbF$_6^-$.** In the same way as described above, the reaction of terthiophene **1**(3T)[21] (20.0 mg, $4.09 \times 10^{-2}$ mmol) and $NO^+SbF_6^-$ (10.9 mg, $4.09 \times 10^{-2}$ mmol) was conducted in $CH_2Cl_2$ to give the salt **1**(3T)$^{\bullet+}SbF_6^-$ (24.1 mg, 72.6%) as dark blue crystals: mp 247.0−250.4 °C (dec); UV−vis ($CH_2Cl_2$) $\lambda_{max}$ (log $\epsilon$) = 586 (4.60), 920 nm (4.60).

**Generation of 1(2T)$^{2+}$.** Bithiophene **1**(2T)[21] (7.10 mg, $2.17 \times 10^{-2}$ mmol) was placed in an NMR tube which was attached as a sidearm to a Pyrex glass tube connected to a vacuum line, while $SbF_5$ (ca. 0.05 mL, 0.7 mmol) was placed in the Pyrex tube under a stream of argon. The tube was immediately evacuated with cooling by liquid nitrogen. $CD_2Cl_2$ (0.75 mL), which had been dried over $CaH_2$ and degassed by three freeze−pump−thaw cycles, was vapor-transferred directly into the cooled Pyrex glass tube. The whole apparatus was sealed under vacuum, and the solution of $SbF_5$ in $CD_2Cl_2$ was added to **1**(2T) in the NMR tube. The color of the solution immediately turned to red after mixing, and then the NMR tube was sealed off under vacuum. The $^1$H and $^{13}$C NMR spectra of the resulting solution were taken at −40 °C, to give the results shown in Figure 7.

**Generation of 1(3T)$^{2+}$.** In the same way, the reaction of terthiophene **1**(3T)[21] (16.8 mg, $3.44 \times 10^{-2}$ mmol) and $SbF_5$ (ca. 0.05 mL, 0.7 mmol) was conducted in $CD_2Cl_2$ to give a dark blue solution, and the NMR spectra of this solution taken at room temerature gave the results shown in Figure 8.

**Synthesis of 1(4T)$^{2+}$(SbF$_6^-$)$_2$.** In the same way as the synthesis of **1**(2T)$^{\bullet+}SbF_6^-$, the reaction of quaterthiophene **1**(4T)[21] (14.7 mg, $2.26 \times 10^{-2}$ mmol) and $NO^+SbF_6^-$ (12 mg, $4.5 \times 10^{-2}$ mmol) was conducted in $CH_2Cl_2$ to give the salt **1**(4T)$^{2+}(SbF_6^-)_2$ (11.7 mg, 46%) as dark blue crystals: mp 73.0−77.5 °C (dec); UV−vis ($CH_2Cl_2$) $\lambda_{max}$ (log $\epsilon$) = 788 (4.85), 712 nm (4.41).

**Synthesis of 1(6T)$^{2+}$(SbF$_6^-$)$_2$.** In the same way as described above, the reaction of sexithiophene **1**(6T)[21] (4.0 mg, $4.1 \times 10^{-3}$ mmol) and $NO^+SbF_6^-$ (2.2 mg, $8.2 \times 10^{-3}$ mmol) in $CH_2Cl_2$ gave the salt **1**(6T)$^{2+}(SbF_6^-)_2$ (4.6 mg, 73%) as dark green crystals: mp 204.7−206.8 °C (dec); UV−vis ($CH_2Cl_2$) $\lambda_{max}$ (log $\epsilon$) = 1158 (4.46), 989 nm (4.26).

**Variable-Temperature UV−Vis−NIR Measurements of 1(2T)$^{\bullet+}$SbF$_6^-$ and 1(3T)$^{\bullet+}$SbF$_6^-$.** A crystal of **1**(2T)$^{\bullet+}SbF_6^-$ (0.381 mg, $6.78 \times 10^{-4}$ mmol) or **1**(3T)$^{\bullet+}SbF_6^-$ (1.46 mg, $1.81 \times 10^{-3}$ mmol) was dissolved in dried and degassed $CH_2Cl_2$ (0.50 mL or 1.0 mL, respectively) under vacuum in a quartz cell ($l$ = 0.01 cm) connected to a vacuum line. The whole apparatus was sealed under vacuum, and the UV−vis−NIR spectra were taken at various temperatures with cooling by the aid of an Oxford cryostat using a flow of cold nitrogen gas.

**X-ray Structural Determination.** The intensity data were collected on a Bruker SMART APEX equipped with a CCD area detector with graphite-monochromated MoKα radiation and graphite monochromator. Frames corresponding to an arbitrary hemispher of data were collected at −150 °C using $\omega$ scans of 0.3°. The structure was solved by direct methods (SHELXTL) and refined by the full-matrix least-squares on $F^2$ (SHELEXL-97). All non-hydrogen atoms were refined anisotropically, and all hydrogen atoms were placed according to AFIX instructions.

**1**(2T)$^{\bullet+}SbF_6^-$: $C_{20}H_{22}F_6S_2Sb$; FW = 562.25, triclinic, $P\bar{1}$, $a$ = 7.680(5) Å, $b$ = 8.211(5) Å, $c$ = 9.594(5) Å, α = 96.716(5)°, $\beta$ = 113.151(5)°, $\gamma$ = 107.298(5)°, $Z$ = 1, $R_1$ = 0.0345, w$R_2$ = 0.0808 ($I > 2\sigma(I)$), GOF = 1.027.

**1**(3T)$^{\bullet+}SbF_6^-\cdot CH_2Cl_2$: $C_{31}H_{34}Cl_2F_6S_3Sb$; FW = 809.41, triclinic, $P\bar{1}$, $a$ = 9.653(5) Å, $b$ = 12.687(5) Å, $c$ = 13.237(5) Å, α = 94.644(5)°, $\beta$ = 100.024(5)°, $\gamma$ = 98.039(5)°, $Z$ = 2, $R_1$ = 0.0606, w$R_2$ = 0.1814 ($I > 2\sigma(I)$), GOF = 1.088.

**1**(4T)$^{2+}(SbF_6^-)_2$: $C_{40}H_{42}F_{12}S_4Sb_2$; FW = 1122.48, triclinic, $P\bar{1}$, $a$ = 7.918(5) Å, $b$ = 9.912(5) Å, $c$ = 13.964(5) Å, α = 109.542(5)°, $\beta$ = 100.177(5)°, $\gamma$ = 97.274(5)°, $Z$ = 1, $R_1$ = 0.0510, w$R_2$ = 0.0807 ($I > 2\sigma(I)$), GOF = 1.002.

**1**(6T)$^{2+}(SbF_6^-)_2\cdot CH_2Cl_2$: $C_{61}H_{64}Cl_2F_{12}S_6Sb_2$; FW = 1531.88, triclinic, $P\bar{1}$, $a$ = 11.197(5) Å, $b$ = 16.574(5) Å, $c$ = 16.880(5) Å, α = 79.113(5)°, $\beta$ = 82.739(5)°, $\gamma$ = 77.222(5)°, $Z$ = 2, $R_1$ = 0.0632, w$R_2$ = 0.1361 ($I > 2\sigma(I)$), GOF = 0.766.

**Acknowledgment.** This work was supported by a Grant-in-Aid for COE Research on Elements Science (No. 12CE2005) from the Ministry of Education, Culture, Sports, Science and Technology, Japan. Computation time was provided by the Supercomputer Laboratory, Institute for Chemical Research, Kyoto University. A.W. thanks JSPS for a Research Fellowship for Young Scientists.

**Supporting Information Available:** X-ray crystallographic data (in CIF format) for crystals **1**(2T)$^{\bullet+}SbF_6^-$, **1**(3T)$^{\bullet+}SbF_6^-\cdot CH_2Cl_2$, **1**(4T)$^{2+}(SbF_6^-)_2$, and **1**(6T)$^{2+}(SbF_6^-)_2\cdot CH_2Cl_2$; Cartesian coordinates and total energies for the optimized structures of all calculated molecules, and calculated $^{13}$C NMR chemical shifts (GIAO/6-31+G(d)//B3LYP/6-31G(d)) for **1**(2T)$^{2+}$ and **1**(2T)$^{2+}$. This materials is available free of charge via the Internet at http://pubs.acs.org.

JA039434V